2978 *Chem. Mater.* **2010,** *22,* 2978–2987
DOI:10.1021/cm100372t

CHEMISTRY OF MATERIALS
Article

Processable Multipurpose Conjugated Polymer for Electrochromic and Photovoltaic Applications

Derya Baran,[†,‡] Abidin Balan,[†,‡] Selin Celebi,[†] Beatriz Meana Esteban,[§,∥] Helmut Neugebauer,[§] N. Serdar Sariciftci,[§] and Levent Toppare*[,†,‡]

[†]*Department of Chemistry, and* [‡]*Solar Energy Research and Development Center (GÜNAM), Middle East Technical University, 06531 Ankara, Turkey,* [§]*Linz Institute for Organic Solar Cells (LIOS), Physical Chemistry, Johannes Kepler University of Linz, Austria, and* [∥]*Process Chemistry Centre, c/o Laboratory of Analytical Chemistry, Åbo Akademi University, FIN-20500 Åbo-Turku, Finland*

Received February 5, 2010

A benzotriazole and 3-hexylthiophene (3HT) bearing a donor−acceptor−donor (D-A-D) type conjugated polymer (PHTBT) was synthesized. The polymer is both p and n-dopable, fluorescent, soluble in common organic solvents, and processable. Electrochemical and spectroelectrochemical characterization of PHTBT and its photovoltaic performance in organic bulk heterojunction (BHJ) solar cells (SC) have been measured. Using PHTBT as donor material in BHJ solar cells resulted in increased open circuit voltage (V_{oc}) up to 0.85 V.

Introduction

Conjugated polymers (CPs) will be used in large-scale applications when their processability will be improved and more and more printable electronic applications settle in the market. They attracted attention rapidly in many applications with the increased number of processable materials available and because of their improving electrical and physical properties. New structural designs of conjugated polymers provided fresh air to some fields including; Organic Light Emitting Diodes (OLEDs),[1] Organic Field Effect Transistors (OFETs),[2] Organic Solar Cells (OSCs),[3] and Electrochromic Devices (ECDs).[4]

Polymers that are applicable to many fields are regarded as multipurpose materials offering great potential to lower the cost of active layer production for organic electronics.[5] The attractive properties of CPs are mostly based on the ability to alter the electronic and spectral properties with chemical structural modifications. Tailoring the band gap (Eg) of CPs allows variation in emission wavelength, absorption in the visible region, and the type of charge carriers upon doping.[6]

*To whom correspondence should be addressed. E-mail: toppare@metu.edu.tr. Fax: 90 312 210 32 00. Phone: 90 312 210 32 51.

(1) (a) Kraft, A.; Grimsdale, A. C.; Holmes, A. B. *Angew. Chem., Int. Ed.* **1998**, *37*, 402. (b) Evans, N. R.; Devi, L. S.; Mak, C. S. K.; Watkins, S. E.; Pascu, S. I.; Kohler, A.; Friend, R. H.; Williams, C. K.; Holmes, A. B. *J. Am. Chem. Soc.* **2006**, *128*, 6647. (c) Huang, Q.; Evmenenko, G. A.; Dutta, P.; Lee, P.; Armstrong, N. R.; Marks, T. J. *J. Am. Chem. Soc.* **2005**, *127*, 10227. (d) Tsuji, H.; Mitsui, C.; Sato, Y.; Nakamura, E. *Adv. Mater.* **2009**, *21*, 3776. (e) Zhen, C. G.; Chen, Z. K.; Liu, Q. D.; Dai, Y. F.; Yee Cheong Shin, R.; Chang, S. Y.; Kieffer *J. Adv. Mater.* **2009**, *21*, 2425. (f) Huang, J.; Qiao, X.; Xia, Y.; Zhu, X.; Ma, D.; Cao, Y.; Roncali, J. *Adv. Mater.* **2008**, *20*, 4172. (g) Song, M. H.; Kabra, D.; Wenger, B.; Friend, R. H.; Snaith, H. J. *Adv. Funct. Mater.* **2009**, *19*, 2130.

(2) (a) Fong, H. H.; Pozdin, V. A.; Amassian, A.; Malliaras, G. G.; Smilgies, D. M.; He, M.; Gasper, S.; Zhang, F.; Sorensen, M. *J. Am. Chem. Soc.* **2008**, *130*, 13202. (b) Huang, F.; Chen, K. S.; Yip, H. L.; Hau, S. K.; Acton, O.; Zhang, Y.; Luo, J.; Jen, A. K. Y. *J. Am. Chem. Soc.* **2009**, *131*, 13886. (c) Beaujuge, P. M.; Pisula, W.; Tsao, H. N.; Ellinger, S.; Mullen, K.; Reynolds, J. R. *J. Am. Chem. Soc.* **2009**, *131*, 7514. (d) Pang, S.; Tsao, H. N.; Feng, X.; Mullen, K. *Adv. Mater.* **2009**, *21*, 3488. (e) Cho, S.; Lee, K.; Heeger, A. *J. Adv. Mater.* **2009**, *21*, 1941. (f) Gao, P.; Beckmann, D.; Tsao, H. N.; Feng, X.; Enkelmann, V.; Baumgarten, M.; Pisula, W.; Mullen, K. *Adv. Mater.* **2009**, *21*, 213. (g) McCulloch, I.; Heeney, M.; Bailey, C.; Genevicius, K.; MacDonald, I.; Shkunov, M.; Sparrowe, D.; Tierney, S.; Wagner, R.; Zhang, W.; Chabinyc, M. L.; Kline, R. J.; McGehee, M. D.; Toney, M. F. *Nat. Mater.* **2006**, *5*, 328. (h) Chua, L. L.; Zaumseil, J.; Chang, J. F.; Ou, E. C. W.; Ho, P. K. H.; Sirringhaus, H.; Friend, R. H. *Nature* **2005**, *434*, 194. (i) Irringhaus, H.; Brown, P. J.; Friend, R. H.; Nielsen, M. M.; Bechgaard, K.; Langeveld, B. M. W.; Spiering, A. J. H.; Janssen, R. A. J.; Meijer, E. W.; Herwig, P.; de Leeuw, D. M. *Nature* **1999**, *401*, 685. (j) Horowitz, G. *Adv. Mater.* **1998**, *10*, 365.

(3) (a) Huang, F.; Chen, K. S.; Yip, H. L.; Hau, S. K.; Acton, O.; Zhang, Y.; Luo, J.; Jen, A. K. Y. *J. Am. Chem. Soc.* **2009**, *131*, 13886. (b) Bijleveld, J. C.; Zoombelt, A. P.; Mathijssen, S. G. J.; Wienk, M. M.; Turbiez, M.; de Leeuw, D. M.; Janssen, R. A. J. *J. Am. Chem. Soc.* **2009**, *131*, 16616. (c) Westenhoff, S.; Howard, I. A.; Hodgkiss, J. M.; Kirov, K. R.; Bronstein, H. A.; Williams, C. K.; Greenham, N. C.; Friend, R. H. *J. Am. Chem. Soc.* **2008**, *130*, 13653. (d) Beek, W. J. E.; Sloof, L. H.; Wienk, M. M.; Kroon, J. M.; Janssen, R. A. J. *Adv. Funct. Mater.* **2005**, *15*, 1703. (e) Coakley, K. M.; McGehee, M. D. *Chem. Mater.* **2004**, *16*, 4533. (f) Hoppe, H.; Sariciftci, N. S. *J. Mater. Res.* **2004**, *19*, 1924. (g) Brabec, C. J.; Sariciftci, N. S.; Hummelen, J. C. *Adv. Funct. Mater.* **2001**, *11*, 15. (h) Gunes, S.; Baran, D.; Gunbas, G.; Ozyurt, F.; Fuchsbauer, A.; Sariciftci, N. S.; Toppare, L. *Sol. Energy Mater. Sol. Cells.* **2008**, *92*, 1162. (i) Zoombelt, A. P.; Fonrodona, M.; Wienk, M. M.; Sieval, A. B.; Hummelen, J. C.; Janssen, R. A. J. *Org. Lett.* **2009**, *11*, 903. (j) Colladet, K.; Fourier, S.; Cleij, T. J.; Lutsen, L.; Gelan, J.; Vanderzande, D.; Nguyen, L. H.; Neugebauer, H.; Sariciftci, S.; Aguirre, A.; Janssen, G.; Goovaerts, E. *Macromolecules* **2007**, *40*, 65. (k) Dennler, G.; Sariciftci, N. S. *Proc. IEEE* **2005**, 93.

(4) (a) Sonmez, G.; Sonmez, H. B.; Shen, C. K. F.; Jost, R. W.; Rubin, Y.; Wudl, F. *Macromolecules* **2005**, *38*, 669. (b) Chidichimo, G.; De Benedittis, M.; Lanzo, J.; De Simone, B. C.; Imbardelli, D.; Gabriele, B.; Veltri, L.; Salerno, G. *Chem. Mater.* **2007**, *19*, 353. (c) Gunbas, G. E.; Durmus, A.; Toppare, L. *Adv. Mater.* **2008**, *20*, 691. (d) Gunbas, G. E.; Durmus, A.; Toppare, L. *Adv. Func. Mater.* **2008**, *18*, 2026.

(5) (a) Balan, A.; Baran, D.; Gunbas, G.; Durmus, A.; Ozyurt, F.; Toppare, L. *Chem. Commun.* **2009**, 6768. (b) Thompson, B. C.; Kim, Y. G.; McCarley, T. D.; Reynolds, J. R. *J. Am. Chem. Soc.* **2006**, *128*, 12714.

(6) (a) Roncali, J. *Chem. Rev.* **1997**, *97*, 173. (b) Akoudad, S.; Roncali, J. *Chem. Commun.* **1998**, 2081.

Published on Web 03/24/2010

From the synthetic point of view, the Donor−Acceptor−Donor (D-A-D) route is the most utilized method in terms of diversity in synthetic possibilities while avoiding the solubility limits. The D-A-D approach allows the presence of both electroactive donor groups and electron deficient acceptor unit in the polymer backbone.[6a,7] By this way, the HOMO (highest occupied molecular orbital) of the donor contributes to the polymer's VB (valence band), and the LUMO (lowest unoccupied molecular orbital) of the acceptor moiety contributes to the polymer's CB (conduction band) energy levels. The low lying LUMO of the acceptor unit results in increased tendency to be n-doped.[8]

Polymer BHJ solar cells based on an electron-donating conjugated polymer and an electron-accepting fullerene derivative ([6, 6]-phenyl C_{61} butyric acid methyl ester (PCBM)) offer great potential for the realization of a low-cost, printable and flexible renewable energy source.[9]

Although poly(*p*-phenylene vinylene) (PPV) derivatives were the touchstone in solar cells, introducing poly(3-alkyl thiophenes) (P3AT) to BHJ system triggered a broad research in this area.[10] In the history of organic photovoltaics, P3ATs have been of high interest because of their good solubility, processability, and environmental stability.[11] The red-shifted absorption of a P3AT derivative, poly(3-hexylthiophene) (P3HT), compared to PPVs such as poly[2-methoxy-5-(3′,7′-dimethyloctyloxy)-1,4-phenylene vinylene) (MDMO-PPV) resulted in a 2-fold increase in photocurrent.[12] Hence, photovoltaic devices with 1.5% power conversion efficiencies were obtained.[13] After the realization of these materials' promising potential for highly efficient solar cells, many studies were focused on PATs. Annealing of the P3HT/PCBM active layer in organic solar cells was found to enhance the efficiency[14] with the increased degree of crystallinity.[15] Postproduction treatments such as applying external voltage or thermal treatment led to an overall increase in conversion efficiencies of devices since the free volume and defect density at the interfaces are reduced.[16] The influence of the work function of materials was also studied in organic solar cells to enhance the V_{oc} and thus the efficiency.[17]

As a further step for the development of plastic solar cells, regioregular poly(3-alkylthiophenes) such as poly(3-hexylthiophene) (P3HT), poly(3-octylthiophene) (P3OT), and poly(3-dodecylthiophene) P3DDT were used as electron donors in polymer:fullerene bulk heterojunction solar cells.[18] Moreover, use of chlorobenzene instead of chloroform and toluene as the solvent increased the efficiencies up to 5.1%.[19]

BHJ solar cell performances have been gradually improved, power conversion efficiencies (PCE) of 5−6% have been reported, and different approaches to improve the efficiency of P3HT/PCBM cells are still being reported. However, the relatively small energy difference between the HOMO of P3HT and the LUMO of the fullerene acceptor results in a low open-circuit voltage, $V_{oc} = 0.6$ V[20] which limits the efficiency. This necessitates finding new candidates for further improvements in the field.[21]

Recently, benzotriazole containing donor−acceptor type polymers synthesized in our group showed interesting optoelectronic properties and became great candidates to be used as multipurpose materials in display technologies.[5a,22] Utilizing a benzotriazole unit in the polymer backbone resulted in low LUMO level enabling the polymer to be n-dopable. Here we report electrochromic and photovoltaic characteristics of a benzotriazole and hexylthiophene containing novel donor−acceptor type CP, poly(2-dodecyl-4,7-bis(4-hexylthiophen-2-yl)-2*H*-benzo[*d*][1,2,3]triazole) (PHTBT), as a promising multipurpose material. Electron defficient benzotriazole units introduced in P3HT increased the oxidation potential and resulted in a decrease in the HOMO level of the polymer (−5.50 eV) and an increase in V_{oc} (0.85 V). Optical properties of the polymer utilizing spectroscopic techniques (Photoluminescence (PL), in situ UV−vis−NIR, and in situ FTIR-Attenuated Reflection (ATR) spectroscopy) and its performance in BHJ solar cells as donor material with PCBM as acceptor were investigated.

(7) (a) van Mullekom, H. A. M.; Vekemans, J. A. J. M.; Havinga, E. E.; Meijer, E. W. *Mater. Sci. Eng.* **2001**, *32*, 1.
(8) Thomas, C. A.; Zong, K.; Abboud, K. A.; Steel, P. J.; Reynolds, J. R. *J. Am. Chem. Soc.* **2004**, *126*(50), 16440.
(9) (a) Sariciftci, N. S.; Smilowitz, L.; Heeger, A. J.; Wudl, F. *Science* **1992**, *258*, 1474. (b) Yu, G.; Gao, J.; Hemmelen, J. C.; Wudl, F.; Heeger, A. J. *Science* **1995**, *270*, 1789. (c) Halls, M. J. J.; Walsh, C. A.; Greenham, N. C.; Marseglia, E. A.; Friend, R. H.; Moratti, S. C.; Hons, A. B. *Nature* **1995**, *376*, 498. (d) Kim, J. Y.; Lee, K.; Coates, N. E.; Moses, D.; Nyugen, T. Q.; Dante, M.; Heeger, A. J. *Science* **2007**, *317*, 222.
(10) Lungenschmied, C.; Dennler, G.; Neugebauer, H.; Sariciftci, N. S.; Glatthaar, M.; Meyer, T.; Meyer, A. *Sol. Energy Mater. Sol. Cells.* **2007**, *91*, 379.
(11) Günes, S.; Neugebauer, H.; Sariciftci, N. S. *Chem. Rev.* **2007**, *107*, 1324.
(12) Schilinsky, P.; Waldauf, C.; Brabec, C. J. *Appl. Phys. Lett.* **2002**, *81*, 3885.
(13) Gebeyehu, D.; Brabec, C. J.; Padinger, F.; Fromherz, T.; Hummelen, J. C.; Badt, D.; Schinler, H.; Sariciftci, N. S. *Synth. Met.* **2001**, *118*, 1.
(14) Camaioni, N.; Ridolfi, G.; Casalbore, G. M.; Possamai, G.; Maggini, M. *Adv. Mater.* **2002**, *14*, 1735.
(15) Zhao, Y.; Yuan, G. X.; Roche, P.; Leclerc, M. *Polymer* **1995**, *36*, 2221.
(16) Padinger, F.; Rittberger, R.; Sariciftci, N. S. *Adv. Funct. Mater.* **2003**, *13*, 85.
(17) Frohne, H.; Shaheen, S. E.; Brabec, C. J.; Muller, D. C.; Sariciftci, N. S.; Meerholz, K. *ChemPhysChem* **2002**, *3*, 795.
(18) (a) Reyes, R. R.; Kim, K.; Carroll, D. L. *Appl. Phys. Lett.* **2005**, *87*, 83506-1. (b) Kim, J.; Kim, S.; Lee, H.; Lee, K.; Ma, W.; Huong, X.; Heeger, A. *J. Adv. Mater.* **2006**, *18*, 572.
(19) Hoppe, H.; Sariciftci, N. S. *J. Mater. Chem.* **2006**, *16*, 45.
(20) Park, S. H.; Roy, A.; Beaupre', S.; Cho, S.; Coates, N.; Moon, J. S.; Moses, D.; Leclerc, M.; Lee, K.; Heeger, A. J. *Nat. Photon.* **2009**, *3*, 297.
(21) (a) Li, G.; Shrotria, V.; Huang, J.; Yao, Y.; Moriarty, T.; Emery, K.; Yang, Y. *Nat. Mater.* **2005**, *4*, 864. (b) Ma, W.; Yang, C.; Gong, X.; Lee, K.; Heeger, A. J. *Adv. Funct. Mater.* **2005**, *15*, 1617. (c) Kim, Y.; Cook, S.; Tuladhar, S. M.; Choulis, S. A.; Nelson, J.; Durrant, J. R.; Bradley, D. D. C.; Giles, M.; Mcculloch, I.; Ha, C. S.; Ree, M,. *Nat. Mater.* **2006**, *5*, 197.
(22) (a) Balan, A.; Gunbas, G.; Durmus, A.; Toppare, L. *Chem. Mater.* **2008**, *20*, 7510. (b) Cetin, G.; Balan, A.; Gunbas, G.; Durmus, A.; Toppare, L. *Org. Electron.* **2009**, *10*, 34.
(23) Neugebauer, H. *Macromol. Symp.* **1995**, *94*, 61.

Scheme 1. Synthetic Route to Monomer HTBT and the Polymer PHTBT

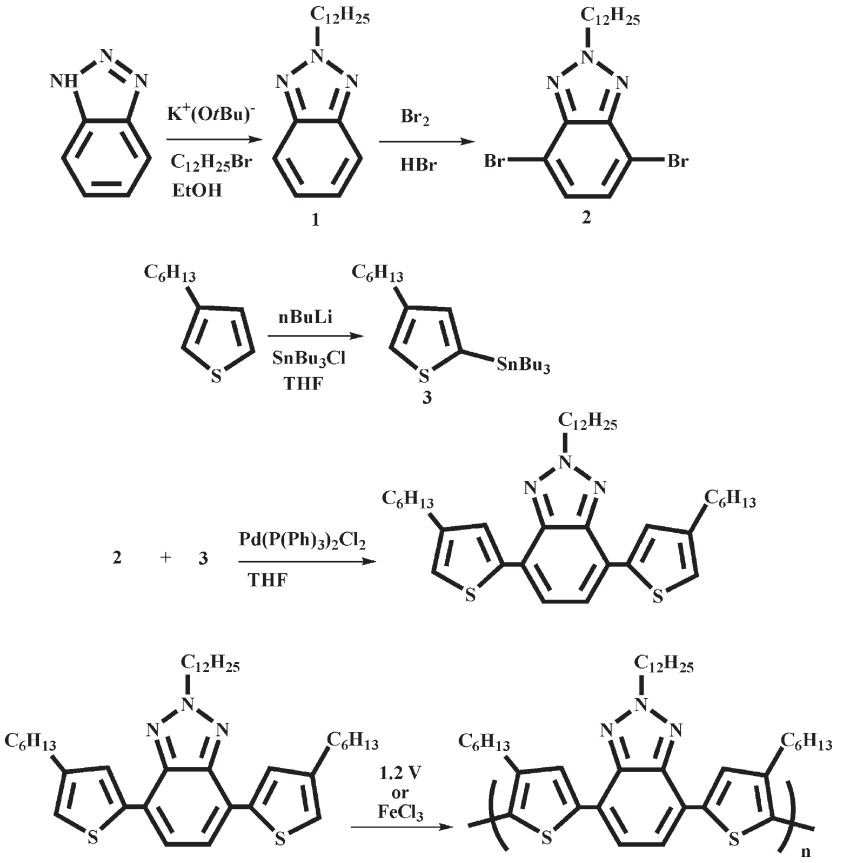

Results and Discussions

Synthesis. Synthesis of the monomer, 2-dodecyl-4,7-bis(4-hexylthiophen-2-yl)-2*H*-benzo[*d*][1,2,3] triazole (HTBT) was performed according to previously reported procedures[5a,22] as shown in Scheme 1. Monomer, HTBT, was obtained via Stille coupling reaction of 2-dodecyl benzotriazole and 3- hexylthiophene. 2-Dodecyl benzotriazole was proved to provide good solubility for the monomer and the polymer in common organic solvents. 2-Position of benzotriazole moiety is serving as a possible functionalization site. It can be functionalized according to the needs. HTBT was polymerized both electrochemically and chemically. The polymer obtained from both polymerizations revealed identical electrochemical and optical properties. However, chemical polymer of PHTBT was used in photovoltaic applications since chemical polymerization allows large scale production.

Table 1 lists the estimated molecular weights from gel-permeation chromatography (GPC) and average number of permeating units. The polymer has high molecular weight and low poly dispersity index (PDI) which means that PTHBT can be synthesized in large scale reproducibly.

Cyclic Voltammetry (CV). HTBT was polymerized potentiodynamically between 0.0 and 1.4 V versus Ag/AgCl quasi reference electrode in a 0.1 M acetonitrile (AN)/tetrabutylammonium hexafluorophosphate ($TBAPF_6$) solution onto ITO coated glass slide to observe the polymer characteristics. During polymerization, a characteristic oxidation peak of monomer was observed at 1.2 V accompanied by a reversible couple for oxidation and reduction of the polymer. In Figure 1, the increase in current density with the number of scans clearly shows the deposition of an electroactive film of PHTBT on ITO. The resultant polymer was soluble in common organic solvents and revealed reversible both p and n doping properties where the p doping/dedoping was indicated by the peaks at 0.9 and 0.5 V respectively. The PHTBT film is orange (Y: 60.1 x: 0.50 y: 0.47) in its neutral state and reveals blue color (Y: 23.0 x: 0.27 y: 0.30) when oxidized.

Oxidation-to-reduction peak ratios were calculated from CV as almost 1.0, which is a clear indication for reversibility of the whole redox process. In literature, 3-hexylthiophene bearing donor−acceptor type molecules have relatively higher polymer oxidation potentials than other common donor units.[24]

In our case, we exploited this property via using PHTBT as the electron donor unit. Since high polymer oxidation potentials and an appropriate band gap result in convenient HOMO−LUMO energy levels, PHTBT can be a strong candidate for p-type photovoltaics.

Oxidation−reduction onset values were determined from CV and Electrochemical Voltage Spectroscopy (EVS). Thus, HOMO−LUMO values for the polymer were estimated from electrochemical data (Table 2). From EVS

(24) (a) Udum, Y. A.; Durmus, A.; Gunbas, G. E.; Toppare, L. *Org. Electron.* **2008**, *9*, 501. (b) Ribeiro, A. S.; Gazotti, W. A., Jr.; dos Santos Filho, P. F.; De Paoli, M. A. *Synth. Met.* **2004**, *145*, 43. (c) Tarkuc, S.; Udum, Y. A.; Toppare, L. *Polymer* **2009**, *50*, 3458.

Table 1. Estimated Molecular Weights of PHTBT from GPC

polymer	M_n	M_w	PDI	av. no. of repeating units
PHTBT	64000	117000	1.81	103

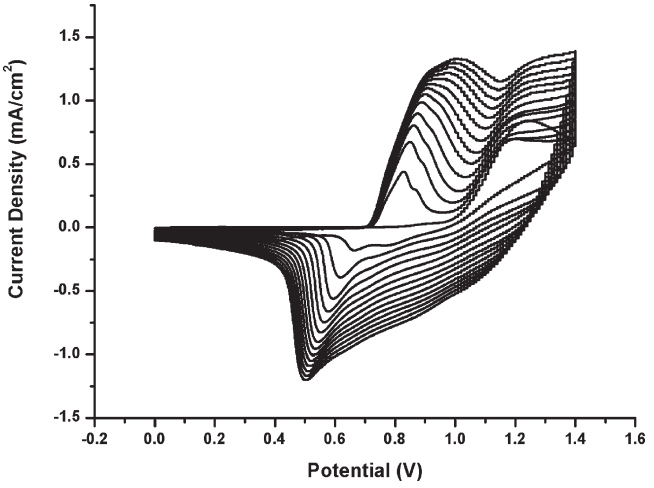

Figure 1. Electrochemical deposition of PHTBT on ITO coated glass slide in a 0.1 M AN/$TBAPF_6$ solvent-electrolyte couple.

experiments, the HOMO and LUMO levels of PHTBT were estimated as −5.45 and −2.95 eV, respectively (the value of NHE was used as −4.75 eV throughout the study[25]). The onset values for both oxidation and reduction obtained from EVS and in CV are in good agreement. The energy levels versus vacuum level were calculated according to the following equations:

$$E_{\mathrm{HOMO}} = -(E_{\mathrm{onset,\,ox}} + 4.75)\ (\mathrm{eV})$$

$$E_{\mathrm{LUMO}} = -(E_{\mathrm{onset,\,red}} + 4.75)\ (\mathrm{eV})$$

$$E^{\mathrm{ec}} = (E_{\mathrm{onset,\,ox}} - E_{\mathrm{onset,\,red}})\ (\mathrm{eV})$$

where by $E_{\mathrm{onset,ox}}$ and $E_{\mathrm{onset,red}}$ represent the onset oxidation and reduction potentials, respectively.

The electrochemical band gap (Eg^{ec}) of PHTBT is higher than the optical gap (Eg^{op}). A similar difference is often observed in conjugated polymers and is usually attributed to the creation of free ions in the electrochemical experiment rather than a neutral excited state.[5b,26]

Figure 2 presents the both p- and n-type doping properties of PHTBT with definite reversible redox couples at 0.9 and 0.6 V for p-type doping and −1.97 V and −1.8 V for n-type doping. Consecutive scans also revealed that the PHTBT can be reversibly oxidized and reduced.

Anodic and cathodic peak currents revealed a linear relationship as a function of scan rate for both p and n-doping, which indicate that the electrochemical processes are not diffusion limited and are reversible even at high scan rates (Figure 3).

Spectroelectrochemistry. *In Situ UV−vis−NIR Characterization*. The behavior of PHTBT upon doping and dedoping was investigated by UV−vis spectroscopy in a monomer free solution containing AN with 0.1 M $TBAPF_6$. The undoped PHTBT film displays an absorption maximum in the visible region at 450 nm which indicates an optical band gap of 1.8 eV (calculated from the onset of the $\pi-\pi^*$ transition for the neutral form). PHTBT is more red-shifted than its thiophene based counterpart and results in a higher band gap.[5a] This can be due to the long alkyl side chains which can induce steric hindrance with adjacent aromatic rings, leading to destroyed chain coplanarity and increased band gap (≥1.8 eV) in thiophene containing donor−acceptor materials.[27]

However; PHTBT can be still considered as a low band gap material for organic photovoltaics. During spectroelectrochemistry, as potential is gradually increased, the peak intensity at 450 nm decreased and new bands at 725 and 1310 nm evolved because of the formation of charge carriers such as polarons and bipolarons,[28] respectively (Figure 4). Upon doping, no charge carriers were formed until 0.75 V. Then a steep increase in the polaronic region was observed which can be interpreted as the oxidation of the polymer film. As seen in CV (Figure 1), no current increase was seen up to 0.75 V which is in accordance with spectroelectrochemical data. A sudden rise in absorbance of polaronic states was recorded at the oxidation potential of the film.[29]

Indications for n-type doping are proved by a reversible redox couple at negative potentials. Additionally and more significantly, a drastic absorption change in the NIR region upon reduction confirms that the polymer is n-dopable. Upon reduction, new bands at around 600 and 1250 nm were formed. The difference in the absorption maxima obtained during oxidation and reduction of the polymer indicate the formation of a polaron and bipolaron.

When the polymer was reduced, a bluish-green (Y: 40.2 x: 0.25 y: 0.29) color was observed, and the increase in the absorbance of nearly 35% in the near-IR region clearly confirmed the formation of charge carriers on the polymer backbone revealing that PHTBT is n-dopable (Figure 5).

In Situ FTIR-ATR Characterization. The oxidation (p-doping) and reduction (n-doping) behavior of PHTBT were studied also by in situ FTIR-ATR spectroscopy. The difference FTIR-ATR spectra recorded during p-doping of the film at 5 mV/s scan rate are shown in Figure 6a. The cyclic voltammogram of the p-doping process is shown as an inset. All spectra are related to a reference spectrum chosen at 0 V where the film is in its neutral state. Figure 6b shows the enlargement of the spectra in the 2000−600 cm^{-1} region. Upon p-doping, a broad increasing

(25) Kötz, E. R.; Neff, H.; Müller, K. *J. Electroanal. Chem.* **1986**, *215*, 33.
(26) (a) Ma, C. Q.; Fonrodona, M.; Schikora, M. C.; Wienk, M. M.; Janssen, R. A. J.; Bauerle, P. *Adv. Funct. Mater.* **2008**, *18*, 3323. (b) Hou, J.; Park, M. H.; Zhang, S.; Yao, Y.; Chen, L. M.; Li, J. H.; Yang, Y. *Macromolecules* **2008**, *41*, 6012. (c) Hou, J.; Tan, Z.; Yan, Y.; He, Y.; Yang, C.; Li, Y. *J. Am. Chem. Soc.* **2006**, *128*, 4911.
(27) Zhang, L.; Zhang, Q.; Ren, H.; Yan, H.; Zhang, J.; Zhang, H.; Gu, J. *Sol. Energy Mater. Sol. Cells.* **2008**, *92*, 581.
(28) Bre'das, J. L.; Chance, R. R.; Silbey, R. *Phys Rev. B* **1982**, *26*, 5843.
(29) Roncali, J. *Chem. Rev.* **1992**, *92*, 711.

Table 2. CV and EVS Results of PHTBT[a]

HTBT	oxidation potential (V)		reduction potential (V)		bandgap (eV)		energy level (eV) from CV		energy level (eV) from EVS	
	E_{ox}	$E_{onset,ox}$	E_{red}	$E_{onset,red}$	Eg^{ec}	Eg^{op}	HOMO	LUMO	HOMO	LUMO
	0.9	0.75	−1.97	−1.8	2.55	1.8	−5.50	−3.0	−5.45	−2.95

[a] CV was recored in 0.1 M AN/$TBPF_6$ at 100 mV/s scan rate.

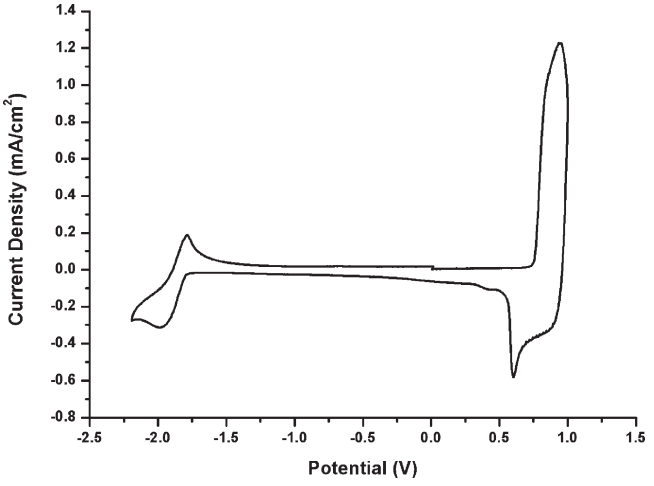

Figure 2. Cyclic voltammogram of PHTBT for both p and n type doping in the presence of 0.1 M AN/$TBAPF_6$.

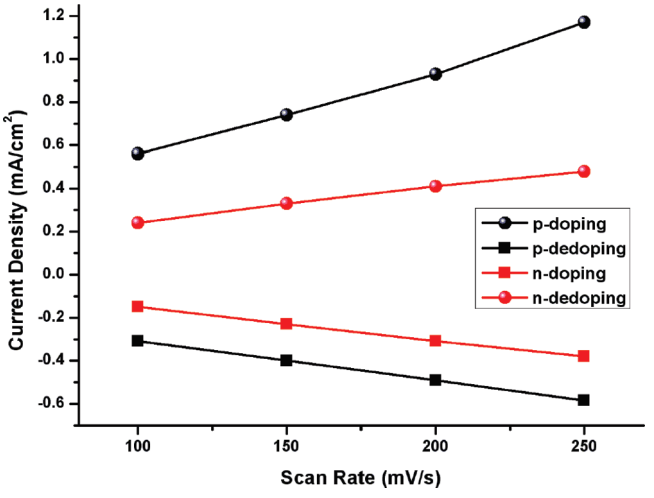

Figure 3. Linear relationship between scan rate and current density of PHTBT film for both p-and n-doping.

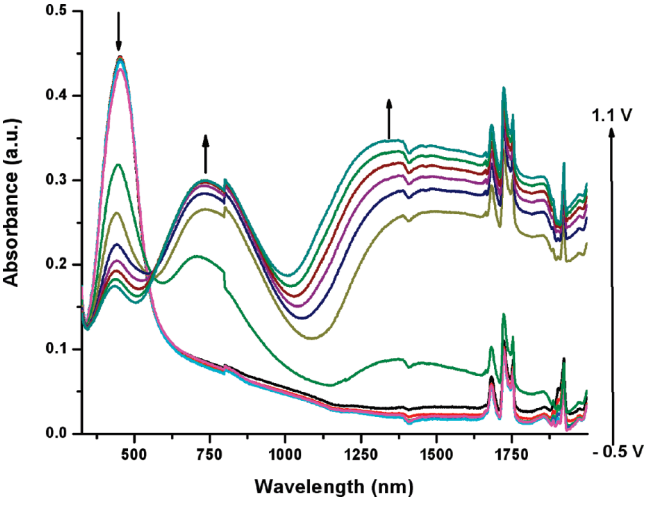

Figure 4. p-Doping electronic absorption spectra of PHTBT between −0.5 and 1.1 V with 0.05 V potential intervals.

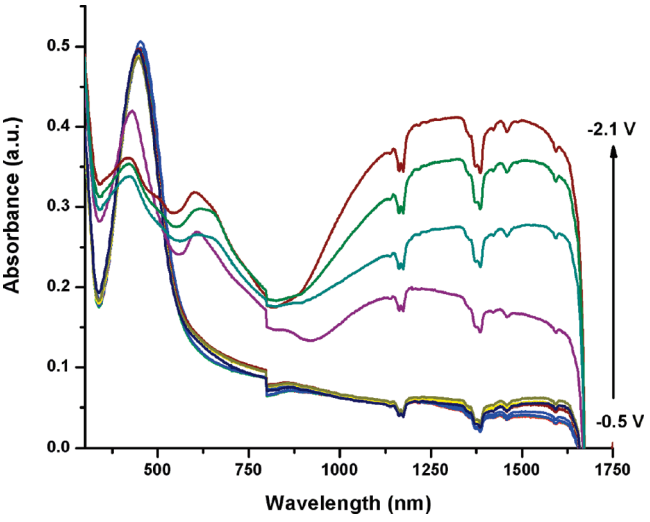

Figure 5. Electronic absorption spectra of PHTBT for n-doping between −0.5 V and −2.1 V with 0.2 V potential intervals.

absorption band above 1500 cm^{-1} appears which is attributed to an electronic transition from the valence band to a new state in the band gap because of the formation of free charge carriers during charging of the film. New doping induced IR bands (IRAV) originating from changes in the conjugated backbone because of the oxidation of the film are found at wavenumbers 1560, 1481, 1370, 1270, 1190, 1145, and 1076 cm^{-1}. The band at 840 cm^{-1} is associated with PF_6^- which results from the insertion of anions into the polymer film during oxidation. The changes in the spectra are fully reversible upon re-reduction of the film to its neutral state.

As stated before, PHTBT can be also electrochemically reduced (n-doped). Figure 7a shows the spectra during electrochemical n-doping at 5 mV/s scan rate. The CV is shown as an inset in Figure 7a. Again, the reference spectrum to which all the subsequent spectra are related is taken at 0 V. From Figure 7a, it can be seen that the electronic absorption related to the formation of free charge carriers during the n-doping process starts to increase at potentials of approximately −1.8 V. Upon further reduction of the film, the electronic absorption band continuously increases and shifts to higher wavenumbers. Figure 7b shows the IRAV bands in the 2000−600 cm^{-1} region. The IRAV bands start to grow at a potential that coincides well with the increase in the intensity of the electronic absorption at higher wavenumbers.

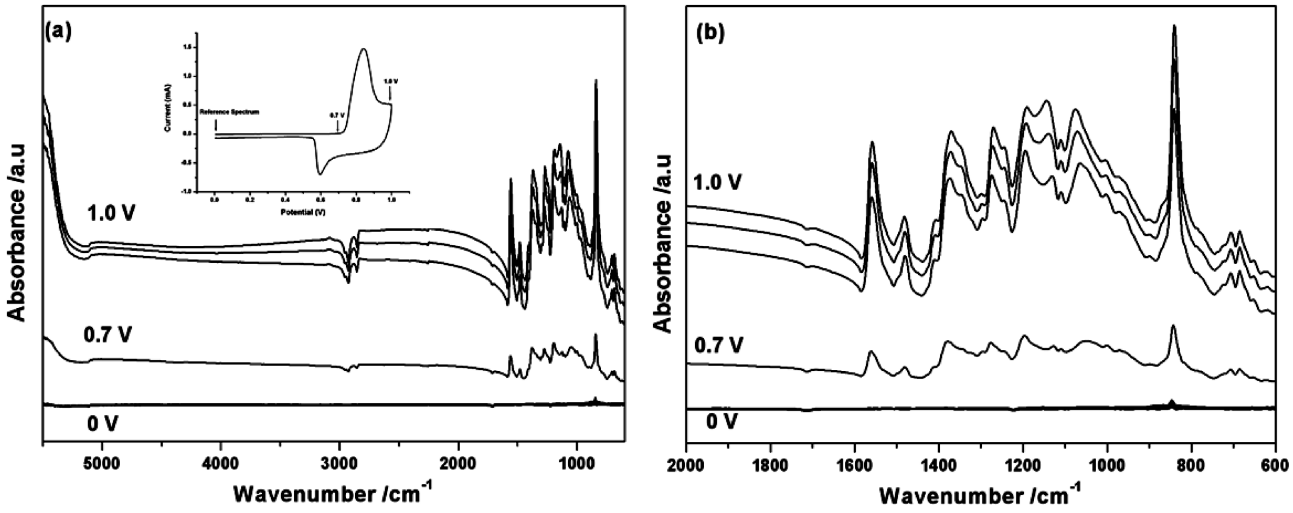

Figure 6. In situ FTIR-ATR spectra recorded during oxidation (p-doping) of a PHTBT film between 0 and 1.0 V (a) in the 5500−600 cm^{-1} region (the potential values where each spectrum was recorded refer to the cyclic voltammogram in the inset and (b) in the 2000−600 cm^{-1} region.

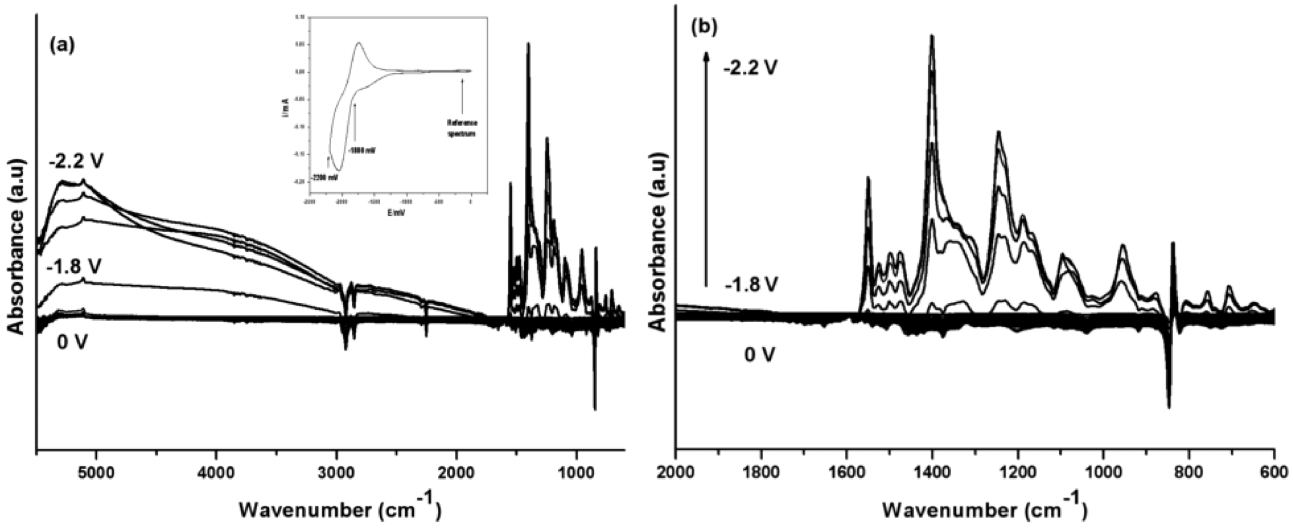

Figure 7. In situ FTIR-ATR spectra recorded during reduction (n-doping) of PHTBT film between 0 and −2.2 V (a) in the 5500−600 cm^{-1} region (the potential values where each spectrum was recorded refer to the cyclic voltammogram in the inset) and (b) in the 2000−600 cm^{-1} region.

The main IRAV bands arising during n-doping appear at 1549, 1399, 1245, 1188, 1095, and 952 cm^{-1}. As seen, the electronic absorption appears at high energies. In addition, the IRAV bands are rather sharp, indicating that the localization of the negative charge carriers along the polymer chain is quite low. As for p-doping, the changes are fully reversible upon reoxidation of the film. From FTIR-ATR experiments, it can be concluded that PHTBT can be reversibly oxidized and reduced; however, the positive and the negative charge carriers have different spectral behaviors and different effective delocalization along the polymer chain. The difference in delocalization of the positive and negative charge carriers has already been reported for other p- and n-dopable polymers.[30]

Optical Studies. Transmittance changes and the switching abilities of the polymer film were determined while sweeping the potentials between oxidized and reduced states. PHTBT revealed 35% transmittance in the visible region at 450 nm. In the near-IR region the optical contrast for the polymer film was found to be 56% which is considerably sufficient for near-IR applications (Figure 8). The long-term switching ability was measured, which is an important parameter for device applications. The polymer film was swept between its oxidized and reduced states via chronoamperometry under the same conditions as in situ UV−vis−NIR spectroscopy. Upon switching, there was less than 10% charge loss even after 1000 full switches.

The absorbance and PL spectra of HTBT in solution and PHTBT both in solution and in thin film form are shown in Figure 9. The lowest energy electronic transition of PHTBT in solution is centered at 498 nm whereas it appears at 473 nm for the film. Emission maxima are at

(30) (a) Kvarnström, C.; Neugebauer, H.; Ivaska, A.; Sariciftci, N. S. *J. Mol. Struct.* **2000**, *521*, 271. (b) Neugebauer, H. *J. Electroanal. Chem.* **2004**, *563*, 153. (c) Meana-Esteban, B.; Kvarnström, C.; Ivaska, A. *Synth. Met.* **2006**, *156*, 426.

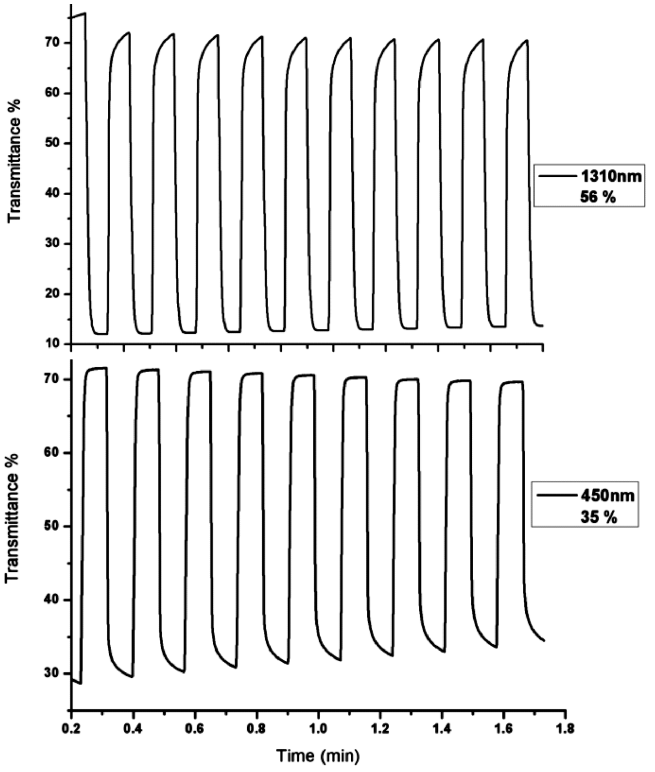

Figure 8. Optical transmittance changes of PHTBT monitored at 450 and 1310 nm while switching the potentials between its oxidized and reduced states.

563 and 592 nm for solution and film, respectively. Long alkyl chains on the polymer backbone, providing high solubility, prevent aggregation, and therefore the Stokes shift was quite low. Absorbance and PL spectra retained similar profiles regardless of the medium. However, because of the increased rigidity in the film form, both absorbance and the emission were blue-shifted with respect to the solution. HTBT revealed two absorption maxima at 283 and 391 nm because of its donor−acceptor nature, and its emission maximum was centered at 464 nm. Emission spectra and also the pictures in Figure 9 show that HTBT and PHTBT are both fluorescent.

BHJ Solar Cell Fabrication and Characterization. PHTBT was designed to act as an electron donor in BHJ photovoltaic devices with PCBM as acceptor. Alkyl chains on the polymer backbone improve the solubility of the polymer in common organic solvents such as chloroform, chlorobenzene and THF. Figure 10 shows the normalized film absorbances of active layers with different PCBM loadings. As the polymer ratio in PHTBT/PCBM mixture decreases (from 1:1 to 1:4), the characteristic peak of PHTBT decreased because of the increase of PCBM amount in the mixture.[31]

The EVS-estimated energy levels of PHTBT were used to construct the energy diagram depicted in Figure 11.

High open circuit voltage obtained for PHTBT can be assigned to the relatively low lying HOMO compared to P3HT.[32]

BHJ photovoltaic cells with ITO/PEDOT:PSS/PHTBT:PCBM/Al (100 nm) configuration [ITO, indium tin oxide; PEDOT, poly(3,4-ethylenedioxythiophene); PSS, poly(styrenesulfonate)] were fabricated and characterized. Charge transfer was confirmed by a quenched PL emission by a factor of 20 when adding 50 wt % PCBM (Figure 12). Such efficient photoluminescence quenching is the proof of ultrafast photoinduced charge transfer from the polymer to PCBM.[33] On the basis of these characterizations, the polymer was expected as an interesting candidate to fabricate photovoltaic devices. Various blends of PHTBT:PCBM with different PCBM content were prepared (1:1, 1:2, 1:3, 1:4 w/w ; 5 mg:10 mg for 1:2) from chlorobenzene solution.

After obtaining the spectral response of the active layers and confirming the charge transfer, the photo induced charge generation was determined. Incident photon to current efficiency (IPCE) is used to get information on the number of photons that contributes to charge generation in a solar cell. Spectral resolved photocurrent measurements showed that the blends generate photoinduced charges nearly over the same range as photons are absorbed in the pristine polymer.[34] In Figure 13, the IPCE spectrum spans from 350 to 900 nm and has a maximum at 450 nm with a peak value of 30% when mixed with PCBM in a ratio of 1:3.

Figure 14 indicates the photovoltaic performance of a series of devices fabricated with different PCBM loadings. The short-circuit current (J_{sc}) increases with increasing PCBM content in the devices and reaches a maximum value of 2.35 mA/cm^2 when the blend ratio is 1:3.

J_{sc} increases from 0.52 mA/cm^2 (for the device containing 50 wt % PCBM) to 2.13 and 2.35 mA/cm^2 for those containing 66% and 75 wt % PCBM. However, J_{sc} decreases for a higher PCBM content (80%) as shown in Figure 14 which means that excess PCBM leads to an imbalanced donor and acceptor ratio.[35] Table 3 summarizes the results obtained from photovoltaic devices with different ratios of PHTBT/PCBM.[36] The lower J_{sc} values compared to P3HT:PCBM devices[20] may stem from a fast recombination of the separated charges, which is a common problem in polymer:fullerene solar cells.[11] However, the performance of PHTBT:PCBM devices may be optimized and/or increased by varying the metal contacts, using LiF as intermediate layer to the Al contact, annealing, changing the active layer composition, film thicknesses, solvent or acceptor material type (C_{70} and its derivatives), and by functionalization of the donor material PHTBT (which may change the absorption

(31) Cook, S.; Ohkita, H.; Kim, Y.; Smith, J. J. B.; Bradley, D. D. C.; Durrant, J. R. *Chem. Phys. Lett.* **2007**, *445*, 276.
(32) (a) Thompson, B. C.; Fre'chet, J. M. J. *Angew. Chem., Int. Ed.* **2008**, *47*, 58. (b) Bundgaard, E.; Krebs, F. C. *Sol. Energy Mater. Sol. Cells* **2007**, *91*, 954. (c) Kroon, R.; Lenes, M.; Hummelen, J. C.; Blom, P. W. M.; Boer, B. *Polym. Rev.* **2008**, *48*, 531. (d) Krebs, F. C. *Sol. Energy Mater. Sol. Cells* **2009**, *93*, 465.
(33) Sariciftci, N. S. *Curr. Opin. Solid State Mater. Sci.* **1999**, *4*, 373.
(34) Muhlbacher, D.; Scharber, M.; Morana, M.; Zhu, Z.; Waller, D.; Gaudiana, R.; Brabec, C. *Adv. Mater.* **2006**, *18*, 2884.
(35) Mayer, A. C.; Scully, S. R.; Hardin, B. E.; Rowell, M. W.; McGehee, M. D. *Mater. Today* **2007**, *10*, 28.
(36) Huang, J. H.; Li, K. C.; Wei, H. Y.; Chen, P. Y.; Lin, L. Y.; Kekuda, D.; Lin, H. C.; Ho, K. C.; Chu, C. W. *Org. Electron.* **2009**, *10*, 1109.

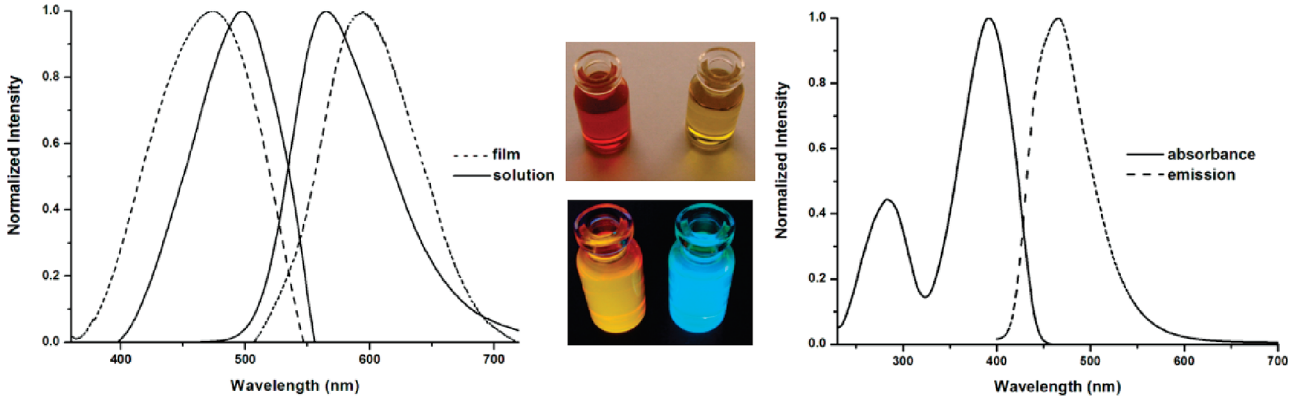

Figure 9. Absorbance and emission spectra of (a) PHTBT in $CHCl_3$ (solid line) and as a thin film (dashed line) (b) HTBT in $CHCl_3$. Pictures of polymer (left) and monomer (right) solutions under daylight and UV lamp (366 nm).

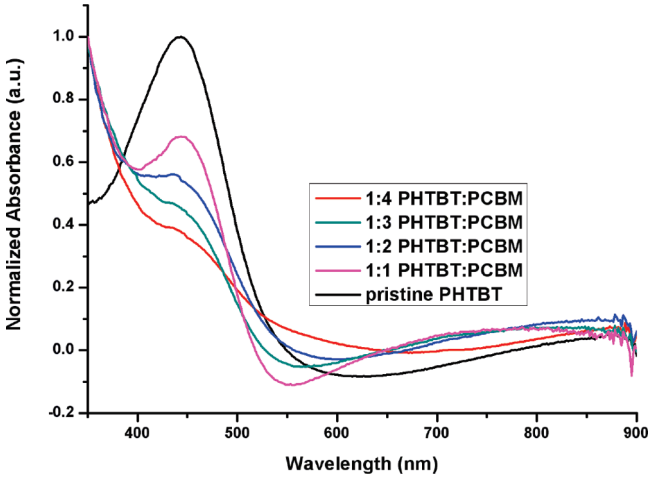

Figure 10. Normalized film absorbance of pristine polymer and mixtures with different PCBM loadings.

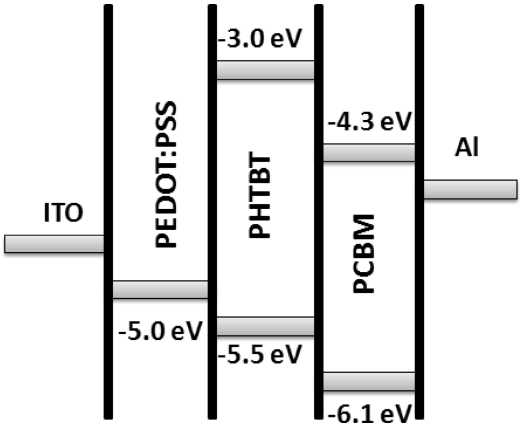

Figure 11. Estimated HOMO−LUMO energy levels for PHTBT and PCBM.

of the active layer and lead to a higher harvesting of photons).

Conclusion

A 3-hexylthiophene and benzotriazole bearing donor−acceptor type conjugated monomer was polymerized both electrochemically and chemically. Its characteristics in electrochromism were investigated with CV, UV−vis−NIR, and PL. PHTBT was found to be both p and n dopable, soluble (both electrochemically and chemically fabricated polymers), processable, and fluorescent. For its device performance in BHJ solar cells, PL, IPCE, and I−V characteristics were studied. The results showed that PHTBT can be a good candidate to obtain high efficient polymeric organic solar cells.

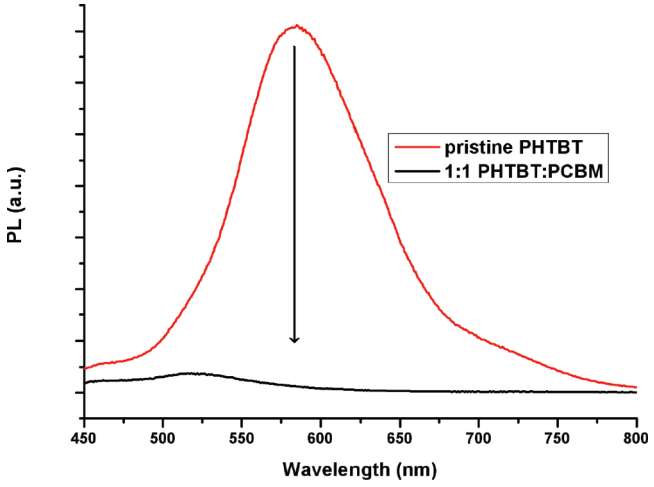

Figure 12. PL quenching of PHTBT upon mixing with PCBM.

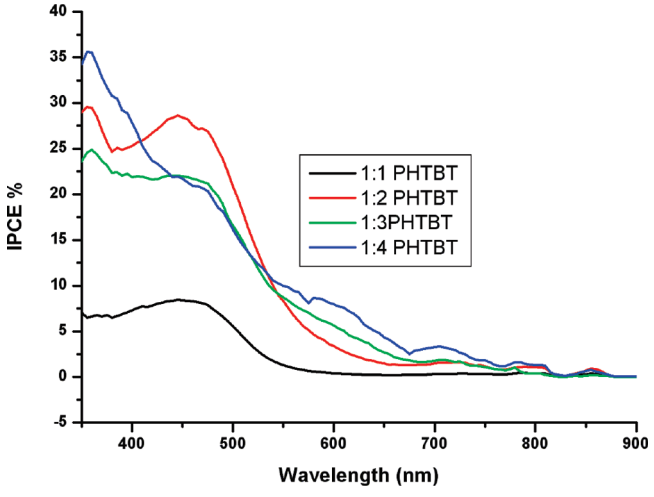

Figure 13. Photocurrent spectra IPCE of photovoltaic devices with PHTBT/PCBM (different ratios) as active layer.

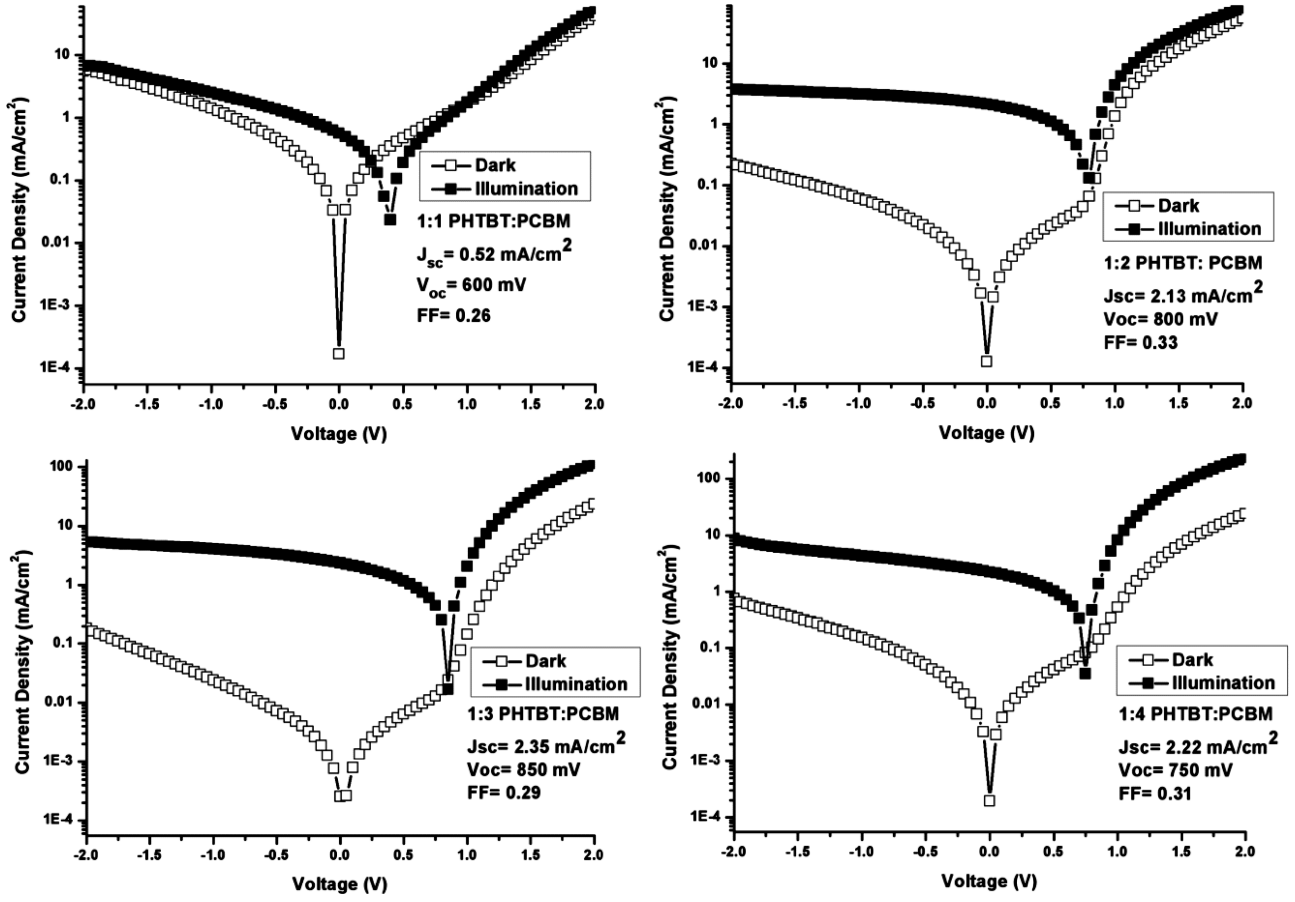

Figure 14. Performance parameters of the measured devices, namely J_{sc} (short-circuit current), V_{oc} (open cicuit voltage), and FF (fill factor) with various PCBM contents under dark and white light illumination (100 mW/cm^2).

Table 3. Photovoltaic Responses Obtained from Solar Cells Containing 1:1, 1:2, 1:3, and 1:4 PHTBT/PCBM Ratio As Active Layer

active layer ratios (PHTBT:PCBM)	open circuit voltage V_{oc} (V)	short circuit current J_{sc} (mA/cm^2)	fill factor FF
1:1	0.6	0.52	0.26
1:2	0.8	2.13	0.33
1:3	0.85	2.35	0.29
1:4	0.75	2.22	0.31

Experimental Section

General Procedures. All chemicals were purchased from Aldrich except THF (tetrahydrofuran) which was purchased from Acros. Tributyl(thiophene-2-yl)stannane was synthesized according to a previously described method.[24a] All reactions were carried out under argon atmosphere unless otherwise mentioned. All electrochemical studies were performed under ambient conditions using a Voltalab 50 potentiostat. Electropolymerization was performed in a three-electrode cell consisting of an Indium Tin Oxide doped glass slide (ITO) as the working electrode, platinum wire as the counter electrode, and Ag/AgCl quasi reference electrode (QRE). The quasi reference electrode (QRE) was a Ag/AgCl wire. After each measurement the QRE was calibrated with ferrocene. The potential of QRE was determined as 50 mV versus the normal hydrogen electrode (NHE). All the data reported in this work are measured against this reference electrode.

^{1}H and ^{13}C NMR spectra were recorded in $CDCl_3$ on a Bruker Spectrospin Avance DPX-400 Spectrometer. Chemical shifts are given in ppm downfield from tetramethylsilane. A Varian Cary 5000 UV−vis spectrophotometer was used to perform the spectroelectrochemical studies of the polymer at a scan rate of 2000 nm/min. The electrochemical voltage spectroscopy (EVS) measurements were carried out at room temperature in a glovebox using a computer controlled potentiostat Jaissle 1030 PC.T. The infrared spectra were recorded with a FTIR spectrometer (Bruker IFS66S) using a Mercury Cadmium Telluride (MCT) detector cooled with liquid nitrogen prior to the measurements. Fluorescence measurements were conducted using a Varian Eclipse spectrofluorometer. Column chromatography of all products was performed using Merck Silica Gel 60 (particle size: 0.040−0.063 mm, 230−400 mesh ASTM). Reactions were monitored by thin layer chromatography using fluorescent coated aluminum sheets. Solvents used for spectroscopy experiments were spectrophotometric grade. Colorimetry measurements were done via a Minolta CS-100 Spectrophotometer. Mass analysis was carried out on a Bruker time-of-flight (TOF) mass spectrometer with an electron impact ionization source. Average molecular weight was determined by gel permeation chromatography (GPC) using a Polymer Laboratories GPC 220.

All current−voltage (I−V) characteristics of the photovoltaic devices were measured using a Keithley SMU 236 under nitrogen in a dry glovebox. A Steuernagel solar simulator for AM 1.5 conditions was used as the excitation source with input power of 100 mW/cm^2 white-light illumination, which was calibrated using a standard crystalline silicon diode. The solar cells were illuminated through the ITO side. The spectrally resolved photocurrent (IPCE) was measured with an EG&G Instruments

7260 lock-in amplifier. The samples were illuminated with monochromatic light of a Xenon lamp.

Synthesis of 2-Dodecylbenzotriazole. 1,2,3-Benzotriazole (5.0 g, 42 mmol), potassium *t*-butoxide (5.0 g, 44 mmol), and bromododecane (12.2 g, 49 mmol) were dissolved in methanol (50 mL). After 12 h, solvent was removed by evaporation, the residue extracted with $CHCl_3$ and water, then dried over $MgSO_4$. Column chromatography on silica gel was performed to obtain 2-dodecylbenzotriazole as a colorless oil (3.7 g, 31%). ^{1}H NMR (400 MHz, $CDCl_3$, δ): 7.76 (m, 2H), 7.26 (m, 2H), 4.62 (t, J = 7.1 Hz 2H), 2.12 (m, 2H), 1.25−1.15 (m, 18H), 0.78 (t, J = 6.0 Hz, 3H); ^{13}C NMR (100 MHz, $CDCl_3$, δ): 144.3, 126.1, 117.9, 56.6, 31.8, 30.0, 29.5, 29.4, 29.4, 29.3, 29.3, 29.0, 26.5, 22.6, 14.0.

Synthesis of 4,7-Dibromo-2-dodecylbenzotriazole. 2-Dodecylbenzotriazole (3.7 g, 13.1 mmol) in aqueous HBr solution (5.8 M, 15 mL) was stirred for 1 h at 100 °C. Bromine (5.9 g, 36 mmol) was added, and the mixture was stirred for 12 h at 135 °C. After cooling the mixture to room temperature, an aqueous solution of $NaHCO_3$ was added, and the product was extracted with $CHCl_3$. With column chromatography, 4,7-dibromo-2-dodecylbenzotriazole was obtained as light yellow oil (4.3 g, 75%). ^{1}H NMR (400 MHz, $CDCl_3$,): 7.36 (s, 2H), 4.60 (t, J = 7.0 Hz, 2H), 2.10 (m, 2H), 1.38−1.12 (m, 18H), 0.80 (t, J = 6.9 Hz, 3H). ^{13}CNMR (100 MHz, $CDCl_3$,): 143.7, 129.4, 109.9, 57.4, 31.8, 30.1, 29.5, 29.5, 29.4, 29.4, 29.3, 28.9, 26.4, 22.6, 14.0.

Synthesis of 2-Dodecyl-4,7-bis(4-hexylthiophen-2-yl)-2H-benzo[d][1,2,3]triazole (*HTBT*). 4,7-Dibromo-2-dodecylbenzotriazole (100 mg, 0.224 mmol), and tributyl(4-hexylthiophen-2-yl)stannane were dissolved in THF (100 mL) and dichlorobis-(triphenylphosphine)-palladium(II) (50 mg, 0.045 mmol) was added at room temperature. The mixture was refluxed for 12 h under argon atmosphere. Solvent was evaporated under vacuum, and the crude product was purified by column chromatography on silica gel to obtain 95 mg (68%) HTBT. ^{1}H NMR (400 MHz, $CDCl_3$,): 7.9 (s, 2H), 7.5 (s, 2H), 6.9 (s,2H), 4.8 (t, J = 7.0 Hz, 2H), 2.1 (m, 2H), 1.4−1.1 (m, 18H), 0.9 (t, J = 6.9 Hz, 3H); ^{13}C NMR (100 MHz, $CDCl_3$,): 143.1, 140.1, 138.3, 127.1, 122.4, 121.3, 119.0, 55.5, 30.6, 30.5, 29.5, 29.2, 28.8, 28.4, 28.2, 27.8, 25.49, 21.4, 12.8 MS (m/z): 619 [M+]

Chemical and Electrochemical Polymerization of HTBT. A 150 mg portion of HTBT was dissolved in 20 mL of $CHCl_3$ under argon atmosphere. $FeCl_3$ (156 mg) in 20 mL of nitromethane was slowly added to the monomer solution. The mixture was stirred for 12 h and then added into 200 mL of methanol. The precipitate was filtered, dissolved in $CHCl_3$, and extracted with water. Solvent was removed, and residue was dissolved in 50 mL of THF and 50 mL of hydrazine monohydrate/water (1:1) were added. To reduce the polymer to neutral form, the mixture was stirred for 12 h. THF was evaporated under reduced pressure. Chloroform was added, and the organic phase separated. Solvent was evaporated, and the residue was stirred in acetone to remove unreacted monomers. The polymer was filtered and dried under vacuum to give PHTBT as orange solid. ^{1}H NMR (400 MHz, $CDCl_3$,): 8.0 (thiophene), 7.6 (benzotriazole), 4.8 (N−CH_2), 2.7, 2.2, 1.3, 0.9 (pendant alkyl chain). For electrochemical polymerization, anodic electropolymerization of the monomer was performed in dichloromethane (DCM) and acetonitrile (AN) mixture (5/95, v/v) with 0.1 M $TBAPF_6$ (tetrabutylammonium hexafluorophosphate) supporting electrolyte. ITO coated glass slides, Pt wire and Ag wire were used as working, counter and pseudo reference electrodes, respectively. The polymer coated on ITO was swept between 0 and 1.4 V potentiodynamically.

In Situ FTIR-Attenuated Total Reflection (*FTIR-ATR*) *and EVS*. For the FTIR-ATR and EVS experiments the materials were drop cast from a chlorobenzene solution onto a Ge crystal and a Pt plate respectively. A 0.1 M electrolyte solution of $TBAPF_6$ in AN was used. The electrolyte solution was kept in the glovebox filled with nitrogen to avoid moisture and oxygen during the electrochemical processes. The FTIR measurements were carried out in a small-size ATR spectroelectrochemical cell made from Teflon. The experimental set up for the in situ FTIR-ATR technique was described earlier.[23] The reflection element, Ge crystal served as the working electrode together with a Pt disk and Ag/AgCl as the counter and the quasi-reference electrode, respectively, in a three-electrode electrochemical cell. Before mounting, Ge was polished with diamond paste (1 and 0.25 μm) and rinsed in a reflux system with acetone for 30 min. The cell used for FTIR-ATR measurements was filled by a continuous flow. The cell was previously sealed with paraffin to avoid leakage. In the in situ FTIR-ATR measurements, the redox response of PHTBT was studied by recording the FTIR spectra during slow potential scans with 5 mV/s. For each spectrum 32 interferograms were co-added covering a range of about 80 mV. The resolution was 4 cm^{-1}. The spectra were related to a reference spectrum chosen according to the CV response of the film.

For solar cell preparation, as substrates, glass sheets of 1.5 × 1.5 cm^2 covered with ITO (Merck KG Darmstadt) were used with an ITO thickness of about 120 nm with a sheet resistance of $< 15\ \Omega$. The ITO was patterned by etching with an acid mixture ($HCl/HNO_3/H_2O$ (4.6:0.4:5)) for 30 min. The part of the substrate which forms the contact was covered with a scotch tape to prevent etching. The tape was removed after etching, and the substrate was then cleaned with acetone and iso-propanol in an ultrasonic bath. An aqueous solution of poly(3,4-ethylenedioxythiophene):poly(styrenesulfonate) (PEDOT:PSS) was spin coated on the glass−ITO substrate, and dried under dynamic vacuum. The blends for the active layer with 1:1, 1:2, 1:3, or 1:4 (w:w) ratios of PHTBT/PCBM were prepared by dissolving 5 mg of PHTBT and 10 mg of PCBM (in the case of 1:2)/mL in chlorobenzene (CB) and overnight stirring at 50 °C . For the top electrode 100 nm of aluminum (Al) was thermally evaporated.

The incident photon to current efficiency (% IPCE) was calculated according to the following equation:

$$\mathrm{IPCE}(\%) = (I_{sc} \times 1240)/P_{in} \times \lambda_{incident}$$

where I_{sc} (mA/cm^2) is the measured current under short-circuit conditions of the solar cell. P_{in} (W/m^2) is the incident light power, measured with a calibrated silicon diode, and λ (nm) is the incident photon wavelength.

Acknowledgment. The authors thank European Science Foundation (ESF), TUBA, GÜNAM, and the EC (project number MRTN-CT-2006-035533, SolarNtype) for financial supports, and Assoc. Prof. Serap Gunes for valuable discussions. B.M.E. acknowledges the Academy of Finland for financial support.